Paper-Based Electrochemical Sensing Platform with Integral Battery and Electrochromic Read-Out

Hong Liu and Richard M. Crooks*

Department of Chemistry and Biochemistry, Center for Electrochemistry, and Center for Nano- and Molecular Science and Technology, The University of Texas at Austin, 1 University Station, A5300, Austin, Texas 78712-0165, United States

Ⓢ Supporting Information

ABSTRACT: We report a battery-powered, microelectrochemical sensing platform that reports its output using an electrochromic display. The platform is fabricated based on paper fluidics and uses a Prussian blue spot electrodeposited on an indium-doped tin oxide thin film as the electrochromic indicator. The integrated metal/air battery powers both the electrochemical sensor and the electrochromic read-out, which are in electrical contact via a paper reservoir. The sample activates the battery and the presence of analyte in the sample initiates the color change of the Prussian blue spot. The entire system is assembled on the lab bench, without the need for cleanroom facilities. The applicability of the device to point-of-care sensing is demonstrated by qualitative detection of 0.1 mM glucose and H_2O_2 in artificial urine samples.
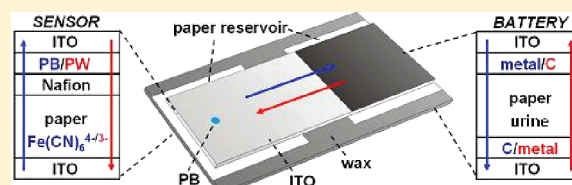
We report a versatile microelectrochemical biosensing platform that is based on paper fluidics and powered by an integral metal/air battery. The battery powers both the sensing chemistry and an electrochromic display that provides an optical indication of the state of the system. The operating voltage of the device is controlled by the identity of the metal foil used in the battery. The sensor is activated by application of artificial urine (AU), which acts both as the matrix for the analyte and the electrolyte for the battery. The entire system is assembled on the lab bench without the need for cleanroom facilities. Taken together, these characteristics suggest the approach described here is appropriate for point-of-care (POC) diagnosis and resource-limited sensing.[1]

Electrochemical methods are widely used for chemical sensing due to their low cost, low power requirements, and simplicity.[2] Most such devices are based on electrolytic reactions and hence require a reader powered by either a battery or line voltage. However, a few self-powered sensors have also been reported.[3−5] The operational basis of the latter devices is a galvanic reaction that is initiated by the presence of an analyte which may or may not itself be redox-active. For example, we recently reported a self-powered sensor in which a galvanic reaction is triggered by the presence of non-electroactive trypsin.[5]

Recently, microfluidic paper analytical devices (μPADs) have emerged as a promising solution to the need for low-cost diagnostic systems.[6] The success of μPADs arises from two main factors: low cost and visual (colorimetric) read-out. However, there is a problem with colorimetric detection: a unique chemistry must be devised and optimized for every reaction. Electrochemical systems provide some relief for this situation, because current replaces the visual read-out signal. This fact has driven the development of microfluidic paper electrochemical devices (μPEDs), which now have the capability of detecting multiple analytes via amperometry.[7,8]

However, the design principle for μPEDs that have been reported thus far involves a disposable paper fluidic system that is controlled and read out using a conventional potentiostat[7,8] or commercial reader.[9,10] Note, however, that in parallel with the development of μPEDs, research in the field of energy storage has resulted in paper-based batteries.[11,12]

The principal advance reported in the present article is a broadly applicable means for fully integrating μPEDs with an inexpensive, on-board power source without giving up the convenience of visual color-based read-out that has driven the field of μPADs. The operational principles of the device are illustrated in Figure 1. The sensor is powered by a metal/air battery that drives electrolytic reactions in a paper reservoir defined by a wax frame. Electrical contact is made to the paper via a pair of transparent indium-doped tin oxide (ITO) electrodes. The paper is preloaded with a dried enzyme and $Fe(CN)_6^{3-}$ or $Fe(CN)_6^{4-}$. The analysis of glucose in AU is carried out as follows. First, glucose in AU is applied to the paper fluidic system, which directs the sample to the reaction zone. Second, glucose oxidase (GOx) present in the paper reaction zone catalyzes glucose oxidation with simultaneous reduction of $Fe(CN)_6^{3-}$ to $Fe(CN)_6^{4-}$. This process activates conversion of electrochromic Prussian blue (PB) on the ITO electrode to colorless Prussian white (PW). As discussed later, a similar approach is used to detect H_2O_2.

■ EXPERIMENTAL SECTION

Chemicals and Materials. ITO electrodes were obtained from Delta Technologies (Loveland, CO) and cut into 25 mm × 10 mm pieces using a glass cutter. Conductive carbon ink,
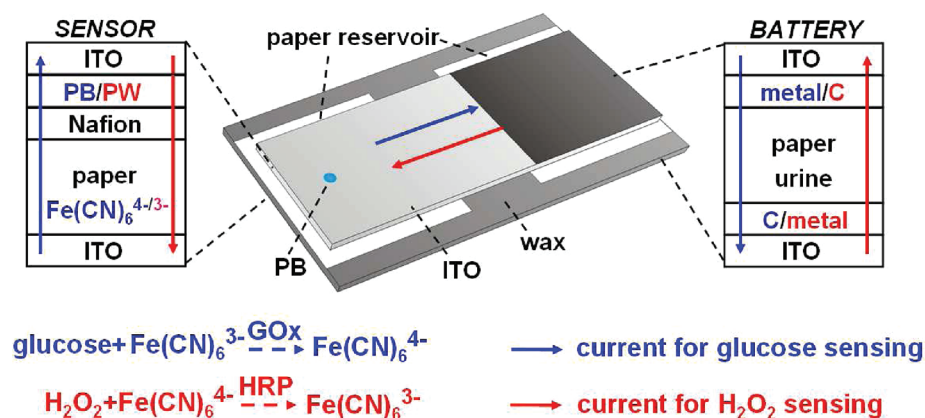
Figure 1. Drawing illustrating the operational principles of the device. The device consists of two parts: a sensor section and an Al/air battery section, which are separated by a wax barrier. For glucose detection, the paper reservoir of the sensor section is preloaded with dried GOx and $Fe(CN)_6^{3-}$. The catalytic oxidation of glucose by GOx results in conversion of $Fe(CN)_6^{3-}$ to $Fe(CN)_6^{4-}$. $Fe(CN)_6^{4-}$ is then oxidized back to $Fe(CN)_6^{3-}$ on the lower ITO electrode, which results in reduction of PB to colorless PW on the upper ITO electrode. The H_2O_2 sensor operation is similar, except that HRP catalyzes the oxidation of $Fe(CN)_6^{4-}$ to $Fe(CN)_6^{3-}$ in the presence of H_2O_2. The resulting $Fe(CN)_6^{3-}$ is then reduced at the lower ITO electrode, while PW is oxidized to PB at the upper ITO electrode. The battery section of the device drives the electrochemical reactions in the sensor section.

thinning solution (Creative Materials, Inc., Tyngsboro, MA), and activated carbon (Sigma-Aldrich) were used to fabricate the battery cathode. Zn, Co, Pb (Alfa Aesar), Cu (Sigma-Aldrich), and Al (Reynolds Wrap, Fisher Scientific) foils were used to fabricate the battery anode. A Sharpie wax pencil (Fisher Scientific) was used for patterning the sensing area on chromatographic paper (grade 1, Whatman). Glucose oxidase was obtained from MP Biomedicals (Solon, OH), and horseradish peroxidase (HRP) was purchased from Sigma-Aldrich. D-Glucose and 30% H_2O_2 solution were obtained from Fisher Scientific. $FeCl_3 \cdot 6H_2O$, $K_3Fe(CN)_6$, and $K_4Fe(CN)_6$ were obtained from Acros Organics. All chemicals necessary for preparing the AU were from Sigma-Aldrich. A Nafion membrane (N-115, Fuel Cell Store, Inc., Boulder, CO) was used to separate the anodic and cathodic reactions in the sensing reservoir while maintaining ionic conductivity. All solutions were prepared with deionized water (18.0 MΩ·cm, Milli-Q Gradient System, Millipore). All reagents were used as received.

Artificial Urine. AU was prepared according to a previously published procedure.[13] It contained 1.1 mM lactic acid, 2.0 mM citric acid, 25 mM sodium bicarbonate, 170 mM urea, 2.5 mM calcium chloride, 90 mM sodium chloride, 2.0 mM magnesium sulfate, 10 mM sodium sulfate, 7.0 mM potassium dihydrogen phosphate, 7.0 mM dipotassium hydrogen phosphate, and 25 mM ammonium chloride. The pH was adjusted to 6.0 using 1.0 M HCl.

Prussian Blue. Electrodeposition of PB on an ITO electrode was carried out as follows. First, a 1 mm thick poly(dimethylsiloxane) (PDMS) slab was prepared by pouring premixed PDMS precursor (Sylgard 184, Dow Corning, Midland, MI) into a plastic Petri dish (Fisher Scientific) and curing at 80 °C in a convection oven for 2 h. Second, a 1.2 mm diameter hole was punched into the slab using a 16 gauge syringe needle to yield a mask. Third, electrodeposition of PB through the mask and onto the ITO was carried out using a previously reported procedure.[14] Briefly, a plating solution containing 2.6 mM HCl, 10 mM $K_3Fe(CN)_6$, and 10 mM $FeCl_3$ was freshly prepared, and then a 100 μL aliquot was dropcast into the hole in the mask. Electrodeposition was

carried out for 60 s at a constant cathodic current of 0.4 μA/mm^2 using a Ag/AgCl reference electrode, a Pt counter electrode, and a CHI 760B potentiostat (CH Instruments, Austin, TX). After deposition, the mask was removed, the ITO electrode was washed with deionized water, and then it was dried under nitrogen gas.

Battery. The battery cathode was fabricated using a mixed carbon material containing 1 g of activated carbon, 4 g of conductive carbon ink, and 2 g of thinning solution. The carbon material was coated onto half of an ITO electrode using a Meyer rod (R.D. Specialties, Inc. Webster, NY). The carbon electrode was then cured at 80 °C in a convection oven for 30 min. The battery anode was fabricated by attaching a piece of metal foil (5 mm × 5 mm) onto an ITO electrode. The open-circuit voltage (OCV) and short-circuit current (SCC) of the batteries were measured using a CHI 760B potentiostat in a two-electrode mode. The SCC was measured with one electrode held at 0 V relative to the other.

Sensors. The paper reservoirs (10 mm × 10 mm) for the sensing and battery modules were fabricated using a wax pencil and a ruler. The hydrophobic walls of the reservoirs were fabricated by drawing on the chromatographic paper using the wax pencil guided by the ruler. The paper was then placed on a hot plate (80 °C for 10 min) to melt the wax so that it penetrated into the paper layer. The paper was then cooled to 20 °C. For glucose sensing, 40 μL of a solution containing 125 mM $K_3Fe(CN)_6$ and 500 U of GOx in 0.01 M PBS buffer (pH 7.4) was dropcast onto the paper electrochemical cell and then dried at 20 °C. For H_2O_2 sensing, 40 μL of a solution containing 125 mM $K_4Fe(CN)_6$ and 100 U of HRP in 0.01 M PBS buffer (pH 7.4) was dropcast onto the paper electrochemical cell and then dried at 20 °C.

The sensors for glucose and H_2O_2 were fabricated by sandwiching the paper, which defined the sensing and battery reservoirs, between two ITO electrodes. A Nafion membrane was used to separate the sensing reagents from the ITO electrode on which the PB or PW spot was immobilized. A binder clip was used to clamp the ITO electrodes so that all layers were in contact with one-another. Electrochemical sensing was initiated after injecting the sample (contained in
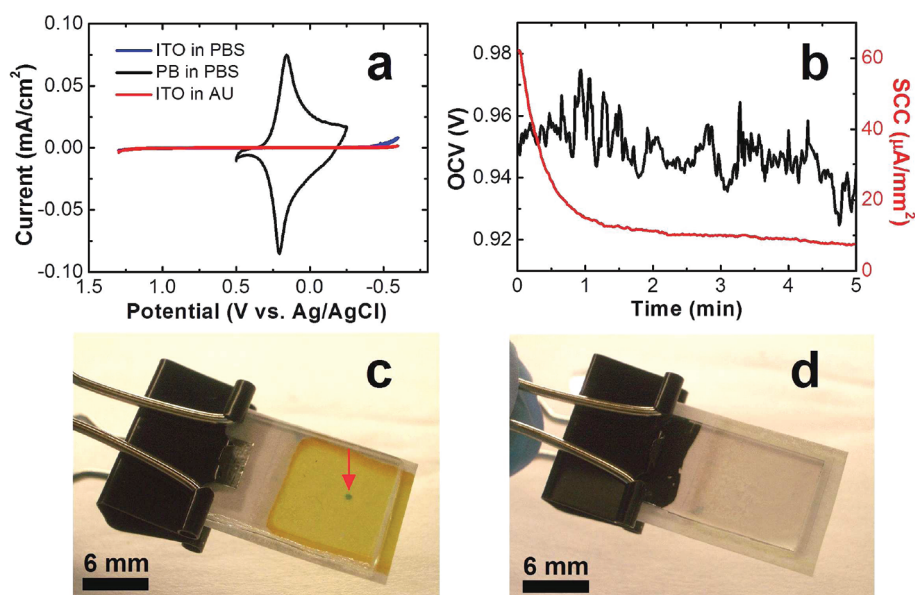
Figure 2. (a) CVs for a naked and a PB-coated ITO electrode in 0.01 PBS buffer (pH 7.4) and a CV for a naked ITO electrode in AU. (b) OCV and SCC measurements for the Al/air battery after activation by AU. (c) A photograph of the battery-powered electrochemical sensor used for glucose detection. A PB dot (diameter = 1.19 mm, indicated by the red arrow) is visible in the sensor region (10 mm by 10 mm, Figure 1) which is surrounded by a wax barrier. The yellow color arises from preloaded $Fe(CN)_6^{3-}$. (d) A photograph of the battery-powered electrochemical sensor used for H_2O_2. The PW dot is colorless so that it is not visible at the sensing area. The binder clip was used to clamp the ITO electrodes together.

AU) into the sensing reservoir. Upon injection of battery electrolyte, the battery was then activated to report the sensing result.

RESULTS AND DISCUSSION

Device Overview. Figure 2a shows cyclic voltammograms (CVs) of ITO electrodes in 0.01 M PBS buffer (pH 7.4) and AU. In both cases no significant current is observed between 1.2 and −0.6 V (vs Ag/AgCl). However, when a thin film of PB is electrodeposited on the ITO electrode,[14] a pair of redox peaks is observed at 0.207 and 0.158 V. These are due to the interconversion of PB (blue) to PW (clear, at more negative potentials).[14]

When one ITO electrode modified with PB or PW is used to construct a two-electrode cell with a second, naked ITO electrode, the reduction of PB to PW can be used to visually report an oxidation reaction occurring on the naked ITO electrode. Likewise, the oxidation of PW to PB can be used to visually report a cathodic reaction on the naked ITO electrode. This is an important property of the device shown in Figure 1, and it is implemented here by separating the anode and cathode with a thin film of Nafion.

As shown in Figure 2c, the PB reporter dot used in this work was 1.19 mm in diameter, and it was electrodeposited on the ITO electrode through a hole punched on a PDMS thin film at a current density of 0.4 $\mu A/mm^2$ for 60 s (24 $\mu C/mm^2$). Unlike some colorimetric reagents, PB is stable indefinitely under ambient conditions. The total charge used to deposit the PB spot for each device reported here was uniform to ensure reproducible color changes. Importantly, the amount of charge stored in the PB or PW spot can be adjusted to match the detection limit and range of the sensor for specific clinical needs. Under optimal conditions, the relationship between the diameter of the PB or PW spot (d in mm) and the lowest

detectable concentration (C in M) of analyte having a particular volume (V in L) is given by eq 1.

$$C = \frac{a\pi d^2 Q}{4nFV} \tag{1}$$

Here, Q is the charge density required for color transition of PB or PW in C/mm^2, n is the number of electrons transferred for the sensing reaction, F is the Faraday constant, and a is a dimensionless empirical constant, which is larger than unity and related to experimental conditions such as sensing time, mass transfer, and enzyme activity. For the devices reported here, C is given by eq 2.

$$C = 4.88 \times 10^{-6} ad^2 = 6.96 \times 10^{-6} a \tag{2}$$

The metal/air battery used in this work was easily fabricated using a piece of metal foil as the anode, high surface area activated carbon as the cathode for oxygen reduction, and paper as the separator. The detailed battery reactions are available in the Supporting Information. The same ITO electrodes used for sensing were used as the current collectors for the battery. The battery was activated immediately prior to sensing by injecting 40 μL of AU onto the paper reservoir. This eliminates the possibility of discharge during long-term storage, and the use of AU as both the battery electrolyte and sample matrix streamlines use of the sensor. Note that activation of a paper-based battery with AU has been reported previously.[15,16] The voltage provided by the battery depends on the identity of the metal-foil anode. As shown in Figure S1 in the Supporting Information, the OCV for batteries, using Zn, Co, Pb, and Cu foils as the anodic materials, were 1.1, 0.68, 0.56, and 0.25 V, respectively, and the SCC increased with increasing battery voltages (Figure S2 in the Supporting Information). In the present study, a 5 mm × 5 mm piece of Reynolds Wrap Al foil was used as the anode for all sensors. The per-sensor cost of the foil is $US 0.00006, and the total cost for each battery, including the ITO current collectors, is $US 0.95. As shown in
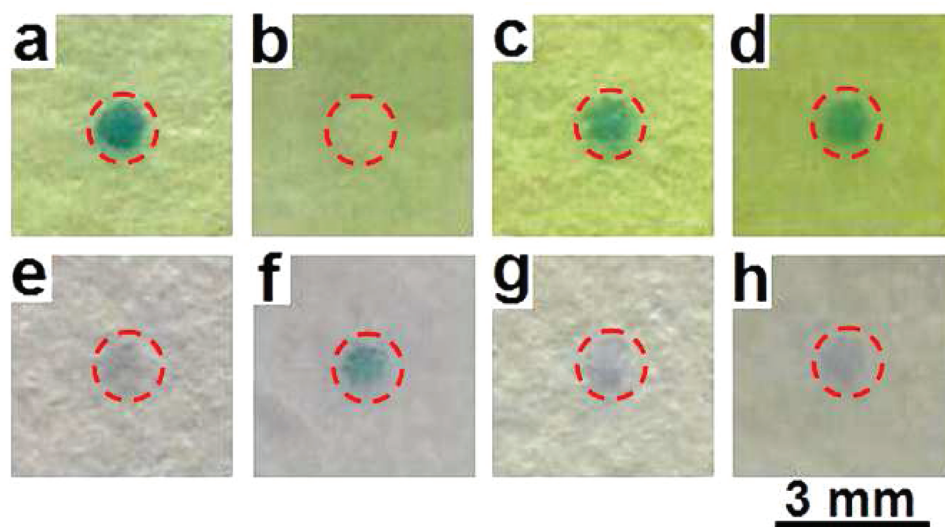
Figure 3. (Top row) Photographs of PB spots (highlighted in red circles) on a glucose sensor (a) before and (b) 50 s after injection of 40 μL of AU containing 0.10 mM glucose. The PB spot turned from blue to colorless due to the presence of glucose. Photographs of a PB spot on a glucose sensor (c) before and (d) 50 s after the injection of 40 μL of glucose-free AU. No color change is observed in the absence of glucose. (Bottom row) Photographs of a PW spot on a H_2O_2 sensor (e) before and (f) 50 s after injection of a 40 μL AU sample containing 0.10 mM H_2O_2. The PW spot turned from nearly colorless to blue due to the presence of H_2O_2. Photographs of a PW spot on a H_2O_2 sensor (g) before and (h) 50 s after the injection of 40 μL of H_2O_2-free AU. No color change is observed in the absence of H_2O_2.

Figure 2b, the average OCV of the Al/air battery was about 0.94 V with a maximum peak-to-peak variation of 50 mV over a period of 5 min. The SCC onset current was 60 μA/mm^2 and decreased to 8 μA/mm^2 after 5 min. For applications other than those described here, it might be advantageous to use different metals in the battery to lower its voltage and thereby avoid background redox processes.

The sensors shown in Figure 2, parts c and d, were configured for detection of glucose and H_2O_2, respectively. The two ITO electrodes were clamped together using a binder clip to ensure reproducible contact between the different layers in the sensor. The top row of micrographs in Figure 3 show the electrochromic reporting areas of a glucose sensor before and after injecting 40 μL of an AU sample containing 0.10 mM glucose. The results from a glucose-free injection are also shown. After injecting the 0.10 mM glucose sample, the PB spot turned from blue to colorless, as shown in Figure 3b. However, under otherwise identical conditions the glucose-free control sample had no effect on the color of the PB spot (Figure 3, parts c and d).

Prior to use of the device for H_2O_2 sensing, the PB spot was reduced to PW (colorless) by holding the potential of the ITO electrode at −0.8 V versus the other ITO electrode for 60 s in 0.01 M PBS buffer (pH 7.4). A slight coloring of the PW spot is present in Figure 3e, and this is due to air oxidation during the device fabrication process. Next, 40 μL AU samples containing 0.10 mM H_2O_2, or a H_2O_2-free solution, were injected onto the paper defining the sensing areas. The color of PW spot turned from nearly colorless to blue for the sample containing 0.10 mM H_2O_2 (Figure 3f), but no color change was observed for the control sample (Figure 3, parts g and h). Videos showing the complete experiments corresponding to the individual frames in Figure 3 are provided in the Supporting Information. The lowest detectable concentration of H_2O_2 and glucose was 0.10 mM, and therefore, according to eq 2, the empirical constant a is 14.4 for these sensors.

SUMMARY AND CONCLUSIONS

We have reported the first paper-based microelectrochemical sensing platform that incorporates an integral power source. The on-board metal/air battery powers both the sensing reactions and the color conversion of the electrochromic spot used for read-out. The voltage provided by the battery is easily controlled by changing the identity of the metal foil, which means that different redox processes can be used for both the sensing chemistry and the electrochromic read-out. The detection limit and dynamic range of the sensor is controlled by matching the amount of charge stored in the PB/PW spot to the clinical threshold values required for different biomarkers. The fabrication of the sensor is very simple and does not require cleanroom facilities. The cost of the sensor, including the integral battery, is very low.

Here we have focused on using the device for obtaining qualitative results. However, studies presently underway are focused on quantitative detection of more realistic biomarkers over a broader range of analyte concentrations. It will also be possible to replace the ITO current collectors in the next generation of this platform so that the entire device is constructed of paper. These enhancements will improve the likelihood that this type of sensing platform will be useful for point-of-care clinical diagnosis and electrochemical sensing under resource-limited conditions.

ASSOCIATED CONTENT

Ⓢ Supporting Information

Additional information about the battery characterization, detailed battery reactions, reactions for sensing, and movies. This material is available free of charge via the Internet at http://pubs.acs.org.

AUTHOR INFORMATION

Corresponding Author

*E-mail: crooks@cm.utexas.edu. Phone: 512-475-8674.

2531

dx.doi.org/10.1021/ac203457h | *Anal. Chem.* 2012, 84, 2528−2532

Notes

The authors declare no competing financial interest.

■ REFERENCES

(1) Gubala, V.; Harris, L. F.; Ricco, A. J.; Tan, M. X.; Williams, D. E. *Anal. Chem.* **2012**, *84*, 487−515.

(2) Wang, J. *Trends Anal. Chem.* **2002**, *21*, 226−232.

(3) Katz, E.; Buckmann, A. F.; Willner, I. *J. Am. Chem. Soc.* **2001**, *123*, 10752−10753.

(4) Germain, M. N.; Arechederra, R. L.; Minteer, S. D. *J. Am. Chem. Soc.* **2008**, *130*, 15272−15273.

(5) Zaccheo, B. A.; Crooks, R. M. *Anal. Chem.* **2011**, *83*, 1185−1188.

(6) Martinez, A. W.; Phillips, S. T.; Whitesides, G. M.; Carrilho, E. *Anal. Chem.* **2010**, *82*, 3−10.

(7) Dungchai, W.; Chailapakul, O.; Henry, C. S. *Anal. Chem.* **2009**, *81*, 5821−5826.

(8) Nie, Z. H.; Nijhuis, C. A.; Gong, J. L.; Chen, X.; Kumachev, A.; Martinez, A. W.; Narovlyansky, M.; Whitesides, G. M. *Lab Chip* **2010**, *10*, 477−483.

(9) Nie, Z. H.; Deiss, F.; Liu, X. Y.; Akbulut, O.; Whitesides, G. M. *Lab Chip* **2010**, *10*, 3163−3169.

(10) Xiang, Y.; Lu, Y. *Nat. Chem.* **2011**, *3*, 697−703.

(11) Hu, L. B.; Choi, J. W.; Yang, Y.; Jeong, S.; La Mantia, F.; Cui, L. F.; Cui, Y. *Proc. Natl. Acad. Sci. U.S.A.* **2009**, *106*, 21490−21494.

(12) Hilder, M.; Winther-Jensen, B.; Clark, N. B. *J. Power Sources* **2009**, *194*, 1135−1141.

(13) Martinez, A. W.; Phillips, S. T.; Whitesides, G. M. *Proc. Natl. Acad. Sci. U.S.A.* **2008**, *105*, 19606−19611.

(14) Itaya, K.; Ataka, T.; Toshima, S. *J. Am. Chem. Soc.* **1982**, *104*, 4767−4772.

(15) Lee, K. B. *J. Micromech. Microeng.* **2005**, *15*, S210−S214.

(16) Lee, K. B. *J. Micromech. Microeng.* **2006**, *16*, 2312−2317.